EVS27 Symposium
Barcelona, Spain, November 17-20, 2013

Sizing the Battery Power for PHEVs Based on Battery Efficiency, Cost and Operational Cost Savings

P. Nelson, R.Vijayagopal, K. Gallagher, A. Rousseau

Argonne National Laboratory, 9700 S Cass Ave, Lemont, IL, USA, nelsonp@anl.gov

Short Abstract

The incremental cost for increasing the power of Li-ion batteries for plug-in hybrid-electric vehicles (PHEVs) is moderate. Hence, the reduction of fuel consumption by using battery power at high vehicle speeds rather than engine power results in high net present value for the total cost of the battery and future fuel savings. The variation of designed efficiency at rated power is also evaluated to examine the cost for the thermal management system and improved life and cold temperature performance. Two types of PHEVs and two lithium-ion battery chemistries of batteries are considered in this study.

Key words: battery model, cost, lithium battery, PHEV, simulation

1 Introduction

1.1 Baseline Vehicle Specifications

The appropriate sizing and utilization of the battery is key to making an efficient PHEV. Over-sizing results in an increased cost and weight of the vehicle, whereas under-sizing might result in higher fuel consumption and diminished value to the consumer. The vehicles included in this study are a PHEV10 with split powertrain configuration and a PHEV40 based on the series PHEV configuration. The vehicles are sized to meet the vehicle technical specifications accepted for the U.S. DRIVE [1] program. It is assumed that the goals set for 2020 in that program for weight reduction and efficiency improvement are accomplished for these two vehicles. Real world driving cycles from the U.S. Environmental Protection Agency (EPA) and survey results from National Highway Traffic Safety Administration (NHTSA) were used to simulate the usage of vehicles over their lifetime [2, 3].

The specifications of the two vehicles used in this study are shown in Table 1. These two vehicles are quite distinct and are sized to meet different operational targets.

Table 1 Vehicle Specifications

Vehicle Specifications		**PHEV10-Split**	**PHEV40-Series**
Engine power	kW	75	75
Motor power	kW	60	113
Generator power	kW	43	75
Battery energy (usable)	kWh	2.0	8.0
Peak battery power	kW	30-90	60-140
Control strategy		Blended	CD + CS
Test weight	kg	1467	1675

The motor power for the PHEV10 vehicle was selected to provide all-electric operation during urban driving (UDDS), whereas the PHEV40 is capable of all-electric operation at highway speeds and on more demanding cycles such as the US06. Within a vehicle type, the powertrain components other than the battery are essentially the same for the entire range of battery power

considered in this study and their costs would be independent of battery power.

1.2 Methodology

This study follows a methodology as illustrated in the Fig 1. The vehicles and drive cycles are defined in Autonomie [4]. Battery characteristics and cost estimates were obtained from BatPaC [5]. A two-time constant battery impedance model was used to determine battery efficiency and internal heating. Simulations over the real world drive cycles provide fuel/electric consumption values. These are compared against the fuel consumption of a conventional vehicle (30 mpg, 7.8 L/100 km). The savings in gasoline is computed over a period of 15 years and 150 thousand miles with a discount rate of 7% for net present value (NPV) calculations. For calculating the net savings for the PHEVs we assumed $4/gallon ($1.06/L) gasoline and $0.10/kWh for electricity. This savings will vary when the battery characteristics of the PHEV are changed.

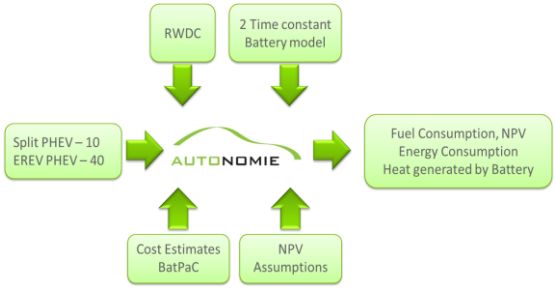

Figure 1: methodology for evaluating the effect of battery power on the NPV of PHEVs

2 Battery Performance and Cost

2.1 Battery Modeling Method

For this study, the vehicle batteries were designed and their costs estimated with a modeling program that utilizes Microsoft® Office Excel spread sheets [5-7]. This program, designated BatPaC, is the product of long-term research and development at Argonne through sponsorship by the U.S. Department of Energy [8-16]. The latest version, BatPaC v2.1, is available from the Argonne website (www.cse.anl.gov/batpac). The bottom-up performance and cost model in BatPaC provides the precise mass and volume of all required battery components necessary to meet the user specified performance. The calculated materials requirements are then directly linked to manufacturing cost calculations that determine both the materials costs and costs associated with manufacturing and overhead. The battery cost includes a warranty so that the full replacement cost is covered for the first five years and shared for the next five years.

The model employs a baseline plant for which the cost of labor, capital equipment, and floor area are estimated for each step in the process. The cost model accounts for different scales of manufacture and different battery designs by recalculating the costs of each manufacturing step. The general approach to cost estimation of multiplying a known cost by the ratio of processing rates raised to a power is applied to each cost item in each step.

Two cell chemistries, NCA-G and LMO-G, which have quite different characteristics, were chosen for this study to illustrate the effects that cell chemistry may have on the cost of batteries for PHEV service. Both cell types have graphite negative electrodes, carbon added to the positive electrode, and binders in both electrodes as is common in the industry. Some pertinent parameters for these cell chemistries are shown in Table 2.

Table 2. Cell material parameters

	NCA-G	LMO-G
Positive Electrode		
Composition of active material	$LiNi_{0.80}Co_{0.15}Al_{0.05}O_2$	$Li_{1.06}Mn_{1.94-x}M'_xO_4$
Capacity, mAh/g of act. Mat.	160	100
Cost of active material, $/kg	33	10
Negative Electrode		
Composition of active material	Graphite (C_6)	Graphite (C_6)
Capacity, mAh/g of act. Mat.	330	330
Cost of active material, $/kg	19	19
Cell OCV at 50% SOC	3.551	3.806
Electrode System ASI		
10-sec burst, ohm-cm^2	23.6	20.0
3-h discharge	51.9	44.0

A cursory review of these data may lead one to believe that the NCA-G system has an advantage in performance because of its relatively high specific capacity, but the higher voltage and lower area-specific impedance (ASI) of LMO-G result in that system having better performance for short-range PHEVs. For a PHEV10, the NCA-G system meets the power requirement for only the lowest powered vehicles in the power range studied and was, therefore, not considered for a PHEV10 battery. The low cost of $Li_{1.06}Mn_{1.94-x}M'_xO_4$ in the LMO-G system is an important advantage.

2.2 Cell and Battery Design Format

The battery design format in BatPaC utilizes a prismatic cell in a stiff-pouch container as shown in Fig. 2.

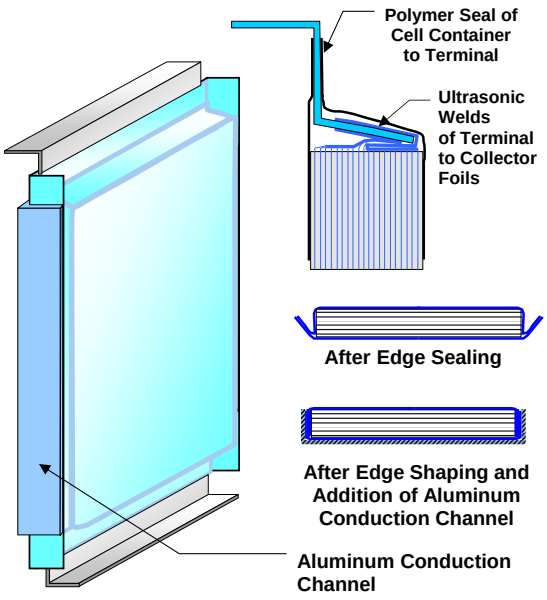

Figure 2. Prismatic cell in stiff pouch container with aluminium conduction channel added for heat rejection from a liquid cooled module

The terminals are almost as wide as the full width of the cell with the positive terminal at one end of the cell and the negative terminal at the opposite end. With this construction, only a very low fraction of the total cell resistance is in the current collection structure. The cells are enclosed in hermetically sealed modules that are cooled on their exterior surfaces by ethylene glycol-water solution, Fig. 3.

The module enclosure protects the cell terminals from the coolant. The modules are enclosed in a battery jacket, which is constructed of a sheet of aluminium on each side of a 10-mm thick layer of ridged, light-weight, high-efficiency insulation. The insulation slows the interaction of the battery with the external environment that cools the battery in the winter and heats it in the summer. Fig. 2 and Fig. 3 show a generic design for the cell and pack, but the actual dimensions for the cells and packs are determined by the specific requirements of this study. Thus, the number of cells for the PHEV10 battery packs was set at 56, which were divided into four modules of 14 cells and the higher power and energy PHEV40 battery packs have 96 cells divided into six modules of 16 cells. The battery packs have dimensions approximately appropriate for installation of the pack under the back seat of a sedan. This was done by arranging the modules in a single row in the battery pack and designing the cells, which lie on a long edge in the pack, with electrodes that have a length-to-width ratio of 3.0.

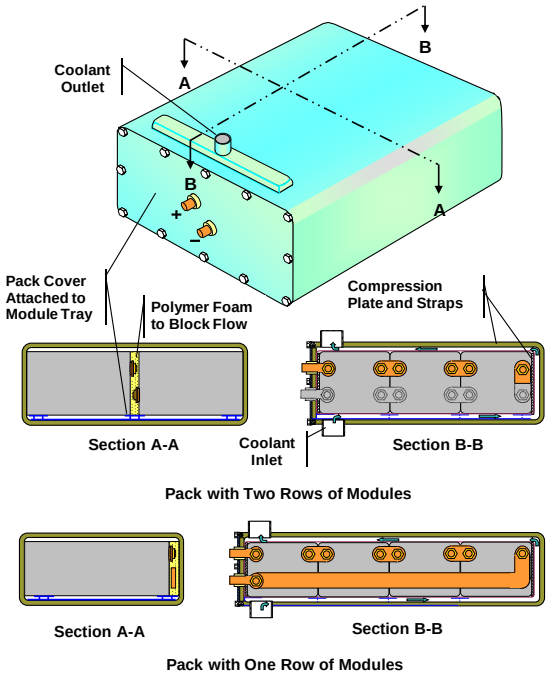

Figure 3. Generic battery pack design in the BatPaC model showing liquid cooling of the exterior of sealed, aluminum-sheet enclosed modules

Three types of vehicle-battery combinations were considered in this study and for each type the energy stored was held constant, but the power was varied over a wide range to study its effect on the costs (Table 3). Within each vehicle type, the volumes and masses of the batteries differ only slightly with change in battery power and all would fit under the back seat of a sedan; no allowance was made for the difference in cost for accommodating the batteries.

2.3 Thermal Management

The pack design shown in Fig. 3 provides cooling with a circulating glycol-water solution, which is cooled to 15°C by means of equipment added to the vehicle air-conditioning system. During

Table 3. Approximate dimensions and masses of battery packs

Battery Pack Parameters	LMOG-split-PHEV10	LMOG-erev-PHEV40	NCAG-erev-PHEV40
Power, kW	30 to 90	60 to 140	60 to 140
Usable energy (70% of total), kWh	2.0	8.0	8.0
Cell capacity, Ah	13.0	30.3	32.7
Number of cells	56	96	96
Number of modules	4	6	6
Length, mm	531-538	897-896	898-896
Width, mm	279-317	394-400	359-401
Height, mm	111-119	149-150	141-150
Volume, L	16.7-20.3	52.8-54.0	45.4-54.0
Mass, kg	26.5-36.0	95.1-99.8	78.6-101.8

driving, the heat generation rate in the battery depends on the vehicle design, the drive cycle and the impedance of the battery. The fluctuations in the temperature of the pack are smoothed out by the battery heat capacity. The rate that the cooling system must handle is the average rate for the most difficult sustained driving conditions to which the battery pack will be subjected.

For vehicle simulation studies with the Autonomie model including determining the heat generation rate for various driving cycles, it was necessary to develop impedance equations for each battery design in the study. For this purpose we selected an equivalent circuit model, which involves a resistance and two capacitance circuits in series that we have used in the past (Fig 4) [17,18]. The polarization time constants τ_1 and τ_2 are 20 s and 270 s, respectively, for the NCA-G system and 15 s and 270 s, respectively, for the LMO-G system.

In preliminary calculations with the Autonomie model, it was found that driving at a constant speed of about 65 mph generated as much battery heating as driving on the US06 driving cycle. The high rate of heat generation at constant speed is caused by the increase in the battery impedance with steady discharge. With the results obtained on Autonomie, a method of calculating the battery power required at constant speed was developed for BatPaC. This method uses the energy requirement for the vehicle on the UDDS cycle (Wh/mile) to estimate the coefficients for rolling friction and aerodynamic drag.

In calculating the cost of the battery packs for this study, the PHEV10 batteries are provided with cooling sufficient for continuous driving at 60 mph, which is above the maximum electric-drive speed for this vehicle. For the PHEV40 batteries, the cooling system is sufficient to withdraw the heat generated during constant speed driving at 75 mph. This provides a significant margin, in that

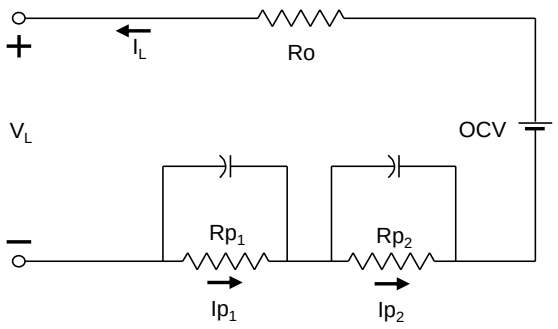

$(OCV-V_L) = R = Ro + Rp_1*Ip_1/I_L + Rp_2*Ip_2/I_L$

$dLp/dt = (I_L - Ip)/\tau$

Where,

OCV = open circuit voltage, V

V_L = cell voltage, V

R = total cell impedance, mohm

Ro = cell internal ohmic resistance, mohm

Rp_1 =1st internal polarization resistance, mohm

Rp_2 = 2nd internal polarization resistance, mohm

IL = cell load current, A

Ip_1 = current through 1st polarization resistance, A

Ip_2 = current through 2nd polarization resistance, A

τ = polarization time constant, s

Figure 4. Impedance model for lithium-ion batteries

the heat stored by the thermal mass of the PHEV40 battery when its temperature rises from 25°C to 35°C is about equal to half of that generated in the battery during discharge of its usable energy for a vehicle driven at 75 mph.

2.4 PHEV10 Batteries

PHEV10 batteries require a high power-to-energy ratio, which could not be met with the NCA-G chemistry except at 30-to 40-kW power, the low end of the power range of interest in this study, at which the batteries were more expensive than the equivalent LMO-G batteries by several hundred dollars. For set energy storage (2.0 kWh useable energy for 10-mile range) the BatPaC model reconfigures the battery for additional power by

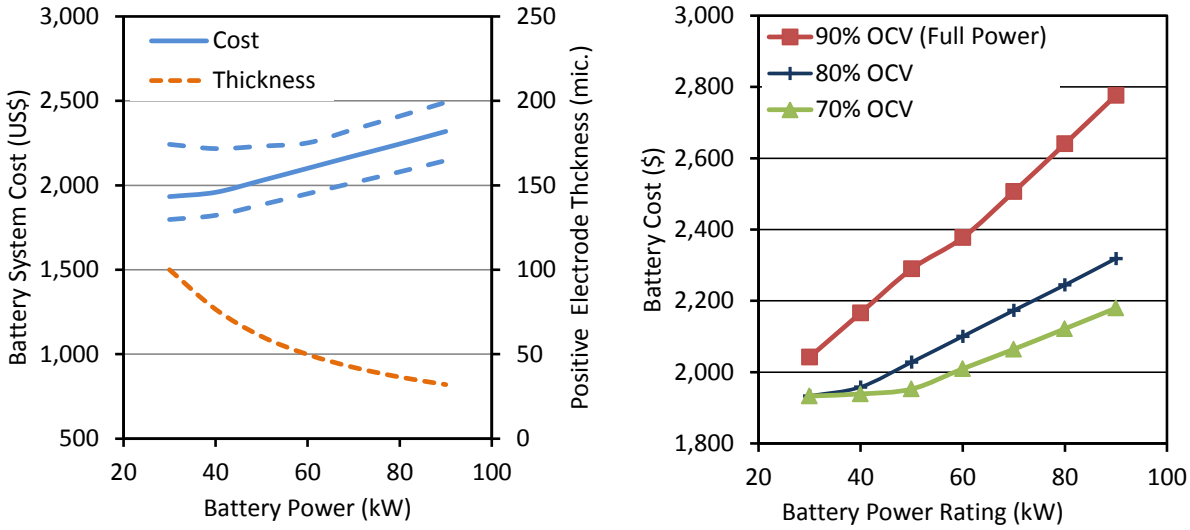

Figure 5. Effects of battery power on total cost to OEM for PHEV10 batteries with LMO-G electrodes and energy requirement of 200 Wh/mile (322Wh/km): a) full power at 80% OCV (showing 95% confidence limits on the cost) and the positive electrode thickness; b) Effect of OCV at full power.

increasing the cell area and decreasing the electrode thicknesses Fig. 5(a). As the cell area increases, the cost of separators, current collector foil and electrode coating increase. Fig. 5(a) also illustrates the determination in BatPaC of the estimated uncertainty in calculating future Li-ion batteries prices, which is discussed in detail elsewhere [7].

The difference between the open-circuit voltage (OCV) and the voltage at which a cell achieves the rated power is one of the most important factors in the design of a battery. The designed voltage at rated power has a direct effect on round-trip battery efficiency, heat removal requirements, cold-cranking power, and allowable power fade. To preserve battery power to the end of life, BatPaC designs the battery to produce the initial rated power at 80% of OCV. This provides for meeting the full rated power after a considerable increase in the battery impedance, although at higher current and higher internal heat generation [6, 7].

For this study, we considered setting the voltage for full power at 70%, 80%, and 90% of OCV (Fig. 5b). For the 70%-OCV battery pack, the cost saving of about $100 compared to the battery producing full power at 80% OCV does not appear to warrant the likely reduction in battery life that would result from the increase in the initial battery impedance. At 90% of OCV, the additional cost for the battery for almost doubling the cell area over that required for reaching full power at 80% of OCV is considerable and sets a strong incentive to develop batteries with relatively stable impedance with battery aging. As a result of these considerations, the batteries reported below for PHEV40 vehicles were all designed to initially provide full power at 80% OCV and with adequate cooling capacity to provide for battery aging effects.

2.5 PHEV40 Batteries

The prices of the PHEV40 batteries (Fig. 6) are higher than those of the PHEV10 batteries (Fig. 5), primarily because of the larger amounts of electrode materials and the additional number of cells required. The lowest powered (60-kW) NCA-G, PHEV40 battery has a negative electrode thickness of 94 microns and the thickness decreases with increasing power (Fig. 6(a)). The cell area also increases with increasing power, to meet the energy requirement with thinner electrodes, resulting in higher cost. The LMO-G batteries have lower ASI, higher voltage and lower specific capacity than the NCA-G batteries (Table 2), resulting in cells of smaller area and thicker electrodes. For LMO-G batteries with power less than 120 kW, the positive electrode thickness is at the limit of 100 microns (Fig. 6(b).

3 Vehicle Simulation Results

The analysis was done with three vehicles, a Split PHEV10 with LMO-G battery, and Series PHEV40 with LMO-G and NCA-G battery models. This was done to show the effects on fuel consumption benefits when battery packs are scaled for different power outputs. Higher battery power benefits these vehicles by enabling more electric operation, which results in reduced fuel consumption is shown in Fig 7.

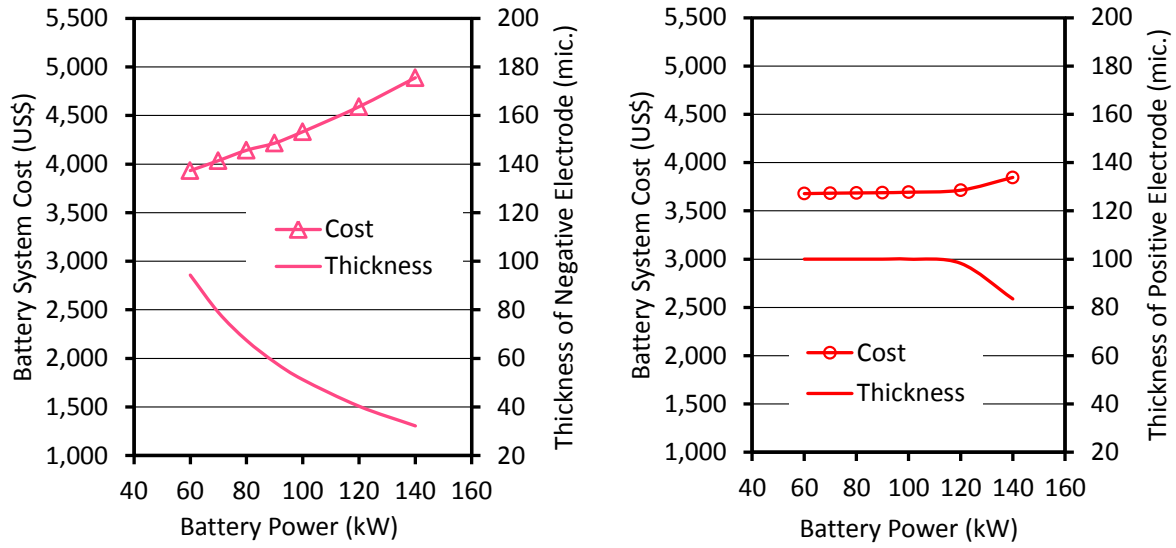

Figure 6. Effects of battery power on total cost to OEM for PHEV40 batteries with energy requirement of 200 Wh/mile: Fig. 6(a) NCA-G electrodes and, b) LMO-G electrodes

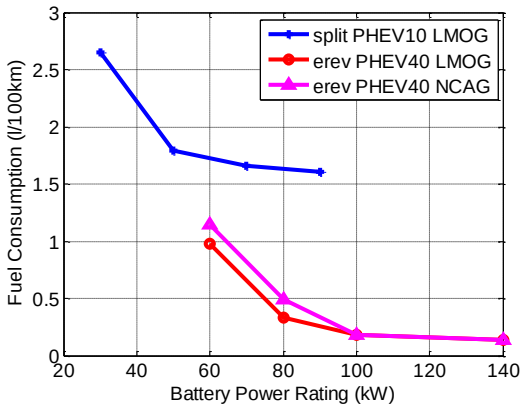

Figure 7. The effect of battery power on fuel consumption

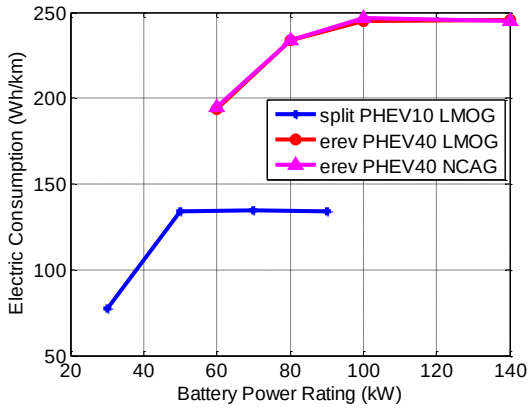

Figure 8. The effect of battery power on electric power consumption

3.1 Electric energy consumption

There are many factors that link the higher battery power to reduced fuel consumption, but the primary reason is the increased use of electric power (Fig. 8). The driving time and distance is fixed in our study, so with higher power batteries, more energy can be discharged/charged during that stipulated period, although this is eventually limited by motor power rating, which was decided based on the minimum operational requirements of the vehicle.

The motor size and the hybrid system efficiencies in these vehicles will determine how much electrical energy can be effectively utilised. These electrical consumption and fuel consumption patterns are applicable only for the sample of real world cycles used for this study. If driving patterns are different, we can expect to see different trends.

3.2 Regenerative braking

Part of the electrical energy used in the vehicle comes from regenerative braking. The battery energy and engine assisted charging controls are fixed for each type of vehicle in this study, so we focused on the effect of battery power on regenerative braking. Higher power and thus higher charging capability for the battery allows more regenerative braking (Fig. 9). The relatively large storage capabilities of these batteries allows effective use of this energy. As the battery charge power increases, it helps to recover a higher percentage of the energy available at the wheel. The charge power is limited in the simulation by the maximum current each battery can handle. It is also limited by the state of charge (SOC) of the battery at the time of braking. The PHEV10 seems to be most successful in utilising the increase in battery power, as it is likely to spend less time at very high SOC region where

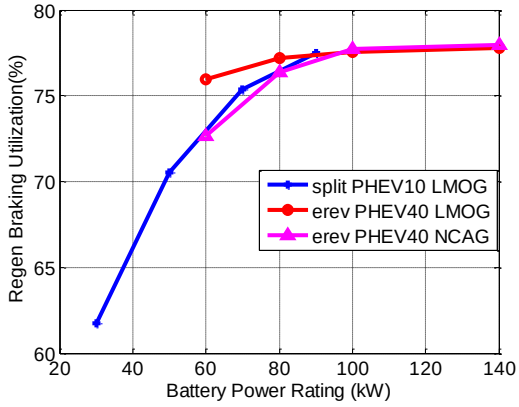

Figure 9. Battery power affects the utilization of regenerative breaking

regenerative braking power is restricted by the vehicle controller.

3.3 Reduced Engine Usage

The reduction in the duration of engine usage also has a significant effect on fuel consumption. This is shown in Fig. 10. For the split PHEV10 there is a drastic reduction in engine on time when battery power increases from ~10-kW to 25-kW. This allows the vehicle to do most city driving with electric power alone. However, the control strategy for a split PHEV10 forces the engine to turn on above a certain speed threshold. This is also evident from the relatively constant 25-minute engine usage (about 20%) observed in Fig 10.

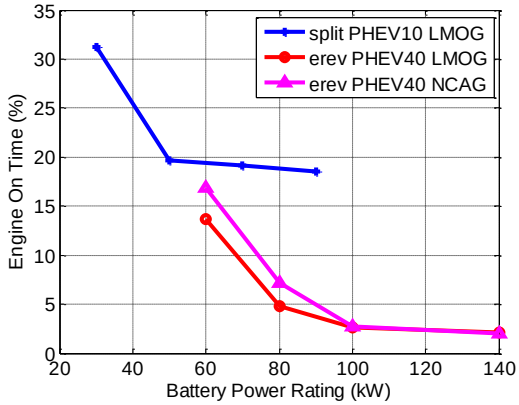

Figure 10. Duration of engine use as a function of battery power

The series PHEV40 has sufficient energy to drive many of the real world drive cycles, however when the battery power is low, the vehicle has to use the engine to supplement the motor power output. As battery power increases, electric drive can be used for most of the cycles. However some cycles are longer than the electric range of the vehicle and will necessitate the use of the engine. These results show that there is a benefit in increased discharge/charge power from the battery. Now the question is whether the gasoline savings obtained by having a more powerful battery justifies the higher cost of the battery.

3.4 Battery Cost

The battery cost estimates were obtained from BatPaC, and the cost varies with battery capacity, power, discharge capability and battery chemistry (Fig. 11). It is interesting that for LMO-G battery chemistry there is a region between 60 and 100 kW, where the cost does not vary with the battery discharge power. This unique characteristic provides an economic incentive to choose the most powerful battery in that power range.

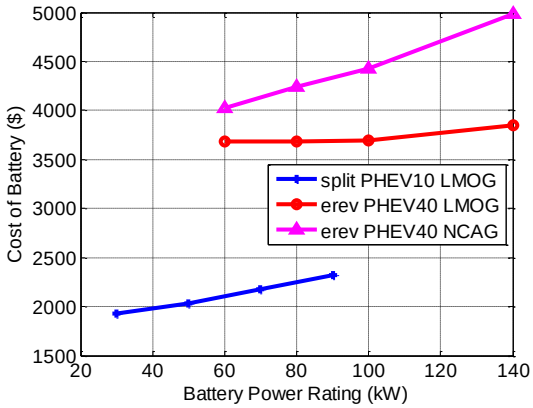

Figure 11. Effect of battery power on battery cost

3.5 Net Present Value of a PHEV Over that of a Conventional Vehicle

The gasoline savings for the different types of PHEVs were evaluated for the lifetime of the vehicles, and the net present value (NPV) was computed as in the process described in earlier studies [7] (Fig. 12).

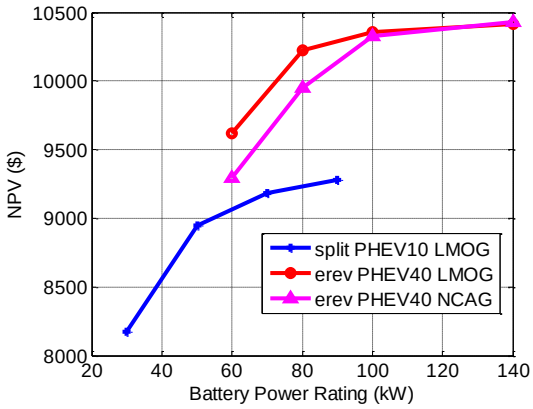

Figure 12. NPV of savings from PHEV operating expenses as a function of battery power

Figure 12 might suggest that the most powerful batteries yield the most savings. However, this plot does not consider the additional investment

needed to purchase a PHEV instead of a comparable conventional vehicle. In other words, the costs of the battery, power electronics and the hybrid powertrain are not factored into this calculation and the costs of all of these components increase when the power rating increases. Among these additional components, we have estimates for the battery cost from BatPaC. The following figure (Fig. 13) illustrates how factoring in the battery cost changes the most favorable battery power choice.

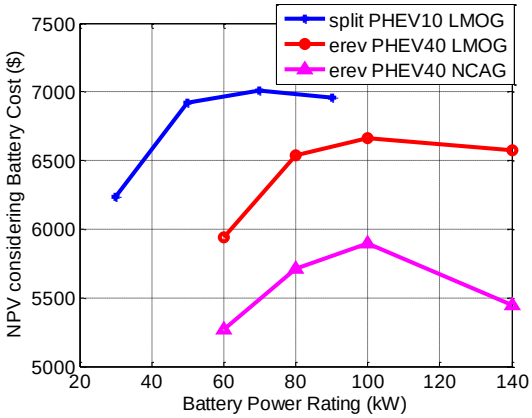

Figure 13. NPV of the PHEV operational costs and the initial battery cost as a function of battery power

This shows that the most value is in having a battery power of about 100-kW, and beyond that there is no justifiable economic return for the additional cost involved. Interestingly the larger power battery provides benefit even to the PHEV10 with a motor rated at 60-kW; this is due to the increased regenerative braking capability discussed earlier.

4 Conclusions

By 2020, the costs to automobile manufacturers for LMO-G batteries of 90-kW power for PHEV10s and of 100-kW power for PHEV40s are expected to be about $2,400 and $3,700 respectively. The NPV of the fuel savings for these vehicles compared to 30-mpg conventional vehicles less the original cost of the batteries was calculated to be about $6,600 for both types of vehicles.

Acknowledgments

This work was supported by DOE's Office of Vehicle Technologies. The support of David Howell, Peter Faguy and David Anderson is gratefully acknowledged. The submitted manuscript has been created by the UChicago Argonne, LLC, Operator of Argonne National Laboratory ("Argonne"). Argonne, a U.S. Department of Energy Office of Science laboratory, is operated under Contract No. DE-AC02-06CH11357. The U.S. Government retains for itself, and others acting on its behalf, a paid-up nonexclusive, irrevocable worldwide license in said article to reproduce, prepare derivative works, distribute copies to the public, and perform publicly and display publicly, by or on behalf of the Government.

References

[1] http://www.uscar.org/guest/about/ accessed on Dec 2012.

[2] Kansas City Real world driving pattern

[3] NHTSA, 'Vehicle Survivability and Travel Mileage Schedules', National Center for Statistics and Analysis, National Highway Traffic Safety Administration, U.S. Department of Transportation, Washington, D.C. 2006.

[4] Argonne National Laboratory, Autonomie, Computer Software, http://www.autonomie.net, accessed on Dec, 2012

[5] P.A. Nelson, K.G. Gallagher, and I. Bloom, BatPaC (Battery Performance and Cost) Software (2012), available from http://www.cse.anl.gov/BatPaC.

[6] P.A. Nelson, K. G. Gallagher, I. Bloom, and D. W. Dees, "Modeling the Performance and Cost of Lithium-Ion Batteries for Electric Vehicles," Chemical Sciences and Engineering Division, Argonne National Laboratory, ANL-11/32, Argonne, IL USA (2011).

[7] P.A. Nelson, K. G. Gallagher, I. Bloom, and D. W. Dees, "Modeling the Performance and Cost of Lithium-Ion Batteries for Electric Vehicles," Second Eddition, Chemical Sciences and Engineering Division, Argonne National Laboratory, ANL-12/55, Argonne, IL USA (2013).

[8] P.A. Nelson, D.J. Santini, J. Barnes, "Factors Determining the Manufacturing Costs of Lithium-Ion Batteries for PHEVs." International Electric Vehicles Symposium EVS-24, Stavanger, Norway, (2009).

[9] D.J. Santini, K.G. Gallagher, P.A. Nelson, "Modeling the Manufacturing Costs of Lithium-Ion Batteries for HEVs, PHEVs, and EVs," International Electric Vehicles Symposium EVS-25, Shenzhen, China, (2010).

[10] K.G. Gallagher, P.A. Nelson, D.W. Dees, "PHEV battery cost assessment" 2011 DOE Merit Review Presentation Washington, DC May 9-12 (2011). Available from http://www1.eere.energy.gov/vehiclesandfuels/pdfs/merit_review_2011/electrochemical_storage/

es111_gallagher_2011_o.pdf (Accessed on July 12, 2011).

[11] P. Nelson, I. Bloom, K. Amine, G. Henriksen, *Journal of Power Sources*, 110, (2002) 437.

[12] P. Nelson, D. Dees, K. Amine, G. Henriksen, *Journal of Power Sources*, 110, (2002) 349.

[13] G.L. Henriksen, K. Amine, J. Liu, and P.A. Nelson, "Materials Cost Evaluation Report for High-Power Li-Ion HEV Batteries," Electrochemical Technology Program, Chemical Technology Division, Argonne National Laboratory, ANL-03/05, Argonne, IL (2002).

[14] P. Nelson, K. Amine, A. Rousseau, H. Yomoto, "Advanced Lithium-Ion Batteries for Plug-in Hybrid-Electric Vehicles", International Electric Vehicles Symposium, EVS-23, Anaheim, Ca (2007).

[15] P. Nelson, "Modeling the Manufacturing Costs of Lithium-Ion Batteries for PHEVs," presented at Plug-in 2009, Long Beach, CA, (2009).

[16] K.G. Gallagher, P.A. Nelson, and D.W. Dees, *Journal of Power Sources*, 196 (2011) 2289.

[17] P. Nelson, J. Liu, K. Amine, G. Henriksen, *ECS Proc. Vol. (F1) POWER Sources Modeling* (2003).

[18] P. Nelson, D. Dees, K. Amine, G. Henriksen, SAE Technical Paper Series, Future Technology Conference , June22-25, 2003.

Authors

Paul A. Nelson is a Senior Chemical Engineer in the Chemical Science and Engineering Division at Argonne National Laboratory and is experienced in battery development and modeling. Paul is a co-creator of the Battery Performance and Cost model (BatPaC). He received his PhD in Chemical Engineering from Northwestern University in 1958 and an MBA degree from the University of Chicago in 1977.Ph.D.

Ram Vijayagopal graduated from the University of Michigan in 2008 with a Master's degree in Mechanical Engineering. He is currently working in Argonne National Laboratory's Vehicle Modeling and Simulation group, where he is involved in the development of Autonomie. Before Argonne, he worked at Hitachi developing motor control algorithms for hybrid electric vehicles, and at Mahindra & Mahindra

Kevin G. Gallagher is a Chemical Engineer in the Chemical Science and Engineering Division at Argonne National Laboratory. Kevin is a co-creator of the Battery Performance and Cost model (BatPaC). His work has also focused on the characterization and modeling of materials and systems for electrochemical energy storage and conversion. He received his PhD in Chemical & Biomolecular Engineering from the Georgia Institute of Technology in 2009.

Aymeric Rousseau is the Manager of the Vehicle Modeling and Simulation Section at Argonne National Laboratory. He received his engineering diploma at the Industrial System Engineering School in La Rochelle, France in 1997. After working for PSA Peugeot Citroen in the Hybrid Electric Vehicle research department, he joined Argonne National Laboratory in 1999 where he is now responsible for the development of Autonomie. He received an R&D100 Award in 2004 and a 2010 Vehicle Technologies Program R&D Award in 2010. He has authored more than 40 technical papers in the area of advanced vehicle technologies.